BIOMOLECULES & THERAPEUTICS

Original Article
Biomol Ther 21(5), 349-357 (2013)

6'-*O*-Galloylpaeoniflorin Protects Human Keratinocytes Against Oxidative Stress-Induced Cell Damage

Cheng Wen Yao, Mei Jing Piao, Ki Cheon Kim, Jian Zheng, Ji Won Cha and Jin Won Hyun*

School of Medicine and Institute for Nuclear Science and Technology, Jeju National University, Jeju 690-756, Republic of Korea

Abstract

6'-O-galloylpaeoniflorin (GPF) is a galloylated derivate of paeoniflorin and a key chemical constituent of the peony root, a perennial flowering plant that is widely used as an herbal medicine in East Asia. This study is the first investigation of the cytoprotective effects of GPF against hydrogen peroxide (H_2O_2)-induced cell injury and death in human HaCaT keratinocytes. GPF demonstrated a significant scavenging capacity against the 1,1-diphenyl-2-picrylhydrazyl (DPPH) free radical, H_2O_2-generated intracellular reactive oxygen species (ROS), the superoxide anion radical (O_2^-), and the hydroxyl radical (•OH). GPF also safeguarded HaCaT keratinocytes against H_2O_2-provoked apoptotic cell death and attenuated oxidative macromolecular damage to DNA, lipids, and proteins. The compound exerted its cytoprotective actions in keratinocytes at least in part by decreasing the number of DNA strand breaks, the levels of 8-isoprostane (a stable end-product of lipid peroxidation), and the formation of carbonylated protein species. Taken together, these results indicate that GPF may be developed as a cytoprotector against ROS-mediated oxidative stress.

Key Words: 6'-*O*-Galloylpaeoniflorin, HaCaT keratinocyte, Hydrogen peroxide, Oxidative stress, Reactive oxygen species

INTRODUCTION

Reactive oxygen species (ROS) (e.g., the superoxide anion radical (O_2^-), singlet oxygen ($^1O_2$), hydrogen peroxide (H_2O_2), and the highly reactive hydroxyl radical (•OH)) are derived from the metabolism of molecular oxygen (Halliwell, 1999). In mammalian cells, potential enzymatic sources of ROS include the mitochondrial electron transport chain, the arachidonic acid-metabolizing enzymes (lipoxygenase and cycloxygenase), the cytochrome P450 enzymes, xanthine oxidase, NAD(P)H oxidases, uncoupled nitric oxide synthase, peroxidases, and other hemoproteins (Cai, 2005). Environmental and dietary pollutants, radiation, and additional metabolic processes can also increase the levels of intracellular ROS (Poljsak, 2011).

Published reports consistently demonstrate a close link among the different kinds of ROS. For example, H_2O_2 is almost always formed under any circumstance where O_2^- is also generated, due to the spontaneous dismutation of O_2^- or its enzymatic dismutation in response to superoxide dismutase (SOD). The direct two-electron reduction of molecular O_2 also contributes to the formation of H_2O_2. This reaction is catalyzed by a number of oxidases that are generally found in the peroxisomes (membrane-bound cytoplasmic organelles) of eukaryotic cells (Farber, 1994). Furthermore, H_2O_2 forms •OH and a hydroxyl anion (OH^-) in the presence of the ferrous ion and other heavy metals as a consequence of the Fenton reaction (Pignatello *et al*., 2006).

Under normal conditions, the cells of aerobic organisms contain safe levels of ROS, which are counterbalanced by biochemical antioxidants. These ROS play a number of important roles in several physiological processes. For instance, ROS are involved in maintaining normal vascular diameter and vascular cell function. They also act together with hypoxia-inducible factor to sense oxygen availability and to initiate appropriate responses for cell survival. In addition, ROS participate in mounting effective immune responses, and they function as possible signaling molecules to regulate glucose uptake in skeletal muscle cells. Furthermore, ROS regulate gene stability and transcription by affecting chromatin stability (Alfadda and Sallam, 2012).

On the other hand, excess ROS generation and/or antioxidant depletion under pathological conditions leads to oxidative stress (Scandalios, 2002), along with direct or indirect ROS-mediated damage to nucleic acids, proteins, and lipids (Ray *et al*., 2012). Cell and tissue defense systems against ROS consist of various antioxidant enzymes (Mn-SOD, Cu/Zn-SOD,

Open Access **http://dx.doi.org/10.4062/biomolther.2013.064**

Received Aug 29, 2013 **Revised** Sep 23, 2013 **Accepted** Sep 24, 2013

***Corresponding Author**
E-mail: jinwonh@jejunu.ac.kr
Tel: +82-64-754-3838, Fax: +82-64-702-2687

extracellular (EC)-SOD, catalase, glutathione peroxidase, and the peroxiredoxins) and non-enzymatic antioxidants (glutathione (GSH), thioredoxin, ascorbate, α-tocopherol, and uric acid) (Pryor, 2000). However, these defense systems are overpowered in the face of high levels of ROS, eventually leading to cell death.

Apoptosis, or programmed cell death, is triggered by a variety of signals and pathophysiological conditions, including ROS-generated oxidative stress (Hampton and Orrenius, 1998). In humans, oxidative stress is thought to be involved in the development of cancer, neurodegeneration, atherosclerosis, diabetes, and aging (Paravicini and Touyz, 2006; Halliwell, 2007; Haigis and Yankner, 2010; Patel and Chu, 2011). Specifically for skin disorders, oxidative stress has been demonstrated to participate in the development of skin carcinoma and skin inflammation. ROS are related to trigger either induction or maintenance of psoriasis, acne, vitiligo, cutaneous allergy, skin aging and varicose ulcer (Bickers and Athar, 2006). Keratinocyte is the predominant cell type in the epidermis, the outermost layer of the skin. Thus, as well as based on all kinds of research, keratinocyte is believed to act as a primary target in a variety of skin disorders. Thus, the inhibition of oxidative stress is theoretically an expeditious method for the management of disorders related to ROS-induced cell injury and apoptosis. The reduction of oxidative stress is achieved at three levels: by lowering exposure to environmental pollutants with oxidizing properties, by increasing levels of endogenous and exogenous antioxidants, and by precluding oxidative stress through the stabilization of mitochondrial energy production and mitochondrial efficiency (Poljsak, 2011). Nonetheless, the employment of antioxidants as therapeutic agents to prevent and cure disease remains controversial, given the ongoing debate in regard to their safety and efficacy. Despite this, antioxidants are currently in widespread use in an attempt to obtain and preserve optimal health (Meyers *et al*., 1996; Brambilla *et al*., 2008).

At present, there is a great deal of interest in the study of natural compounds with free radical scavenging capacity and their role in human health (Srivastava *et al*., 2012). The potential therapeutic benefits of many natural antioxidants have been successfully investigated in vitro and in animal models. For instance, rottlerin, a polyphenol isolated from *Mallotus philippinensis*, inhibits ROS formation and prevents nuclear factor (NF)-κB activation in cultured MCF-7 and HT-29 cells (Maioli *et al*., 2009). Furthermore, curcumin, a widely used yellow pigment obtained from *Curcuma longa*, possesses pronounced antioxidant properties, induces heme oxygenase-1 (HO-1), and protects endothelial cells from oxidative stress

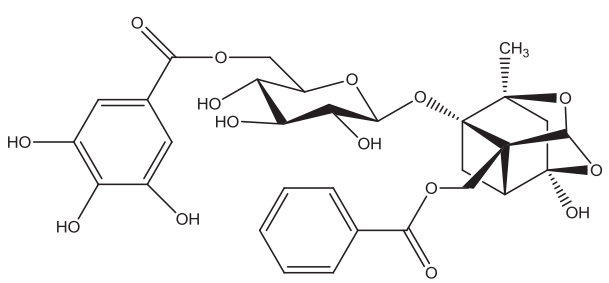

Fig. 1. Chemical structure of 6'-*O*-galloylpaeoniflorin (GPF).

(Motterlini *et al*., 2000). In addition, baicalein, a major flavonoid derived from *Scutellaria baicalensis*, deters H_2O_2-induced oxidative damage and apoptosis in several types of cells (Liu *et al*., 2012).

The current study investigated the antioxidant properties of the natural compound, 6'-O-galloylpaeoniflorin (GPF) and its potential to safeguard skin cells from oxidative stress. Galloylpaeoniflorin is an acylated monoterpene glucoside isolated from the peony root and this compound has three positional isomers and consists of D-glucose, galloyl, and benzoyl moieties (Kang *et al*., 1991). GPF (Fig. 1) is distinguished from the other two galloylpaeoniflorin isomers by the galloyl group at the 6'-position of the glucose moiety. Matsuda *et al*. (2001) reported that GPF is a more potent scavenger of the 1,1-diphenyl-2-picrylhydrazyl (DPPH) radical than α-tocopherol, and also showed that the galloyl group is essential for its free radical scavenging abilities. However, no further investigations regarding the antioxidant characteristics of GPF are available. The present study therefore investigated the cytoprotective function of GPF against H_2O_2-induced ROS generation and cell injury in human HaCaT keratinocytes.

MATERIALS AND METHODS

Reagents

GPF was provided by Professor Sam Sik Kang (Seoul National University, Republic of Korea) as described previously (Kang *et al*., 1991). N-acetyl cysteine (NAC), 5,5-dimethyl-1-pyrroline-N-oxide (DMPO), 2',7'-dichlorodihydrofluorescein di-acetate (DCF-DA), DPPH, (3-(4,5-dimethylthiazol-2-yl-2,5-diphenyltetrazolium) bromide (MTT), and Hoechst 33342 dye were purchased from Sigma Chemical Co. (St. Louis, MO, USA). Diphenyl-1-pyrenylphosphine (DPPP) was purchased from Molecular Probes (Eugene, OR, USA). All other chemicals and reagents were of analytical grade.

Cell culture

The human HaCaT keratinocyte cell line was obtained from Amore Pacific Company (Gyeonggi-do, Republic of Korea) and maintained at 37°C in an incubator with a humidified atmosphere of 5% CO_2/95% air. The cells were cultured in RPMI 1640 containing 10% heat-inactivated fetal calf serum, streptomycin (100 μg/ml), and penicillin (100 units/ml).

Cell viability assay

The effect of GPF on the viability of HaCaT cells was determined via the MTT assay, which is based on the reduction of a tetrazolium salt by mitochondrial dehydrogenases in viable cells. Cells were seeded into a 96-well plate at a density of 1×10^5 cells/ml. Sixteen hours later, the cells were treated with GPF at a concentration of 1, 5, 10, or 20 μM. After a 16 h incubation, MTT stock solution (50 μl, 2 mg/ml) was added to each well to yield a total reaction volume of 200 μl. Four hours later, the supernatants were aspirated. The formazan crystals in each well were dissolved in dimethyl sulfoxide (DMSO, 150 μl), and the absorbance at 540 nm was read on a scanning multi-well spectrophotometer (Carmichael *et al*., 1987).

DPPH radical scavenging activity

GPF (1, 5, 10, or 20 μM) or NAC (2 mM) was added to a solution of DPPH (0.1 mM) in methanol. The resulting reac-

tion mixture was shaken vigorously. After 3 h, the amount of residual, unreacted DPPH was measured at 520 nm by using a spectrophotometer.

Detection of intracellular ROS

The DCF-DA method was used to detect intracellular ROS generated by H_2O_2-mediated oxidation in HaCaT keratinocytes (Rosenkranz *et al*., 1992). HaCaT cells were seeded into 96-well plates at a density of 1.0×10^5 cells/ml. Sixteen hours later, they were treated with GPF (1, 5, 10, or 20 μM) or NAC (2 mM), an established antioxidant employed as the positive control. After a 1-h incubation at 37°C, H_2O_2 (1 mM) was added to the wells, and the plates were again incubated for 30 min at 37°C. At this time, DCF-DA solution (50 μM) was added to each well. Thirty minutes later, the fluorescence of the 2', 7'-dichlorofluorescein (DCF) product was detected and quantified by using a PerkinElmer LS-5B spectrofluorometer (PerkinElmer, Waltham, MA, USA).

Image analysis for the generation of intracellular ROS was conducted by seeding the cells into a four-well plate mounted on a chamber slide at a density of 1×10^5 cells/well. At 16 h after plating, the cells were treated with GPF (20 μM). After 1 h, H_2O_2 (1 mM) was added to the plate and incubated with the cells for 30 min. Next, DCF-DA (100 μM) was added to each well and incubated with the cells for an additional 30 min at 37°C. After washing with phosphate buffered saline (PBS), mounting medium was added to the stained cells, and images were collected by using a confocal microscope and the Laser Scanning Microscope 5 PASCAL program (Carl Zeiss, Jena, Germany).

Detection of the superoxide anion

The superoxide anion was generated by the xanthine/xanthine oxidase system and then reacted with a nitrone spin trap, DMPO (Sigma Chemical Co.). The DMPO/•OOH adducts were detected by using a JES-FA electron spin resonance (ESR) spectrometer (JEOL, Tokyo, Japan) (Kohno *et al*., 1994). Briefly, ESR signaling was recorded 2.5 min after 20 ml of xanthine oxidase (0.25 U/ml) was mixed with 20 μl each of xanthine (10 mM), DMPO (3 M), and GPF (20 μM). The ESR spectrometer parameters were set as follows: magnetic field=336 mT, power=1.00 mW, frequency=9.4380 GHz, modulation amplitude=0.2 mT, gain=500, scan time=0.5 min, scan width=10 mT, time constant=0.03 sec, and temperature=25°C.

Detection of the hydroxyl radical

The hydroxyl radical was generated by the Fenton reaction (H_2O_2+$FeSO_4$) and then reacted with DMPO. The resultant DMPO/•OH adducts were detected by using an ESR spectrometer (Li *et al*., 2004). The ESR spectrum was recorded 2.5 min after a phosphate buffer solution (pH 7.4) was mixed with 0.2 ml each of DMPO (0.3 M), $FeSO_4$ (10 mM), H_2O_2 (10 mM), and GPF (20 μM). The ESR spectrometer parameters were set as follows: magnetic field=336.8 mT, power=1.00 mW, frequency=9.4380 GHz, modulation amplitude=0.2 mT, gain=200, scan time=0.5 min, scan width=10 mT, time constant=0.03 sec, and temperature=25°C.

Nuclear staining with Hoechst 33342

Cells were treated with GPF (20 μM) or NAC (2 mM) for 1 h, followed by the addition of H_2O_2 (1 mM). After further incubation for 24 h at 37°C, the DNA-specific fluorescent dye, Hoechst 33342 (1.5 μl, 10 mg/ml stock), was added to each well and incubated with the cells for 10 min at 37°C. The stained cells were visualized under a fluorescence microscope equipped with a CoolSNAP-Pro color digital camera. The degree of nuclear condensation was evaluated, and the apoptotic cells were quantified.

Single-cell gel electrophoresis (comet assay)

The extent of oxidative DNA damage was determined in an alkaline comet assay (Singh, 2000; Rajagopalan *et al*., 2003). A suspension of HaCaT cells was mixed with 0.5% low-melting agarose (LMA, 75 μl) at 39°C, and the mixture was spread on a fully frosted microscopic slide pre-coated with 1% normal melting agarose (NMA, 200 μl). After solidification of the agarose, the slide was covered with another 75 μl of 0.5% LMA and then immersed in a lysis solution (2.5 M NaCl, 100 mM Na-EDTA, 10 mM Tris, 1% Trion X-100, and 10% DMSO, pH 10) for 1 h at 4°C. The slides were subsequently placed in a gel electrophoresis apparatus containing 300 mM NaOH and 10 mM Na-EDTA (pH 13) for 40 min to allow for DNA unwinding and the expression of alkali labile damage. An electrical field was then applied (300 mA, 25 V) for 20 min at 4°C to draw the negatively charged DNA toward the anode. The slides were washed three times for 5 min each time at 4°C in a neutralizing buffer (0.4 M Tris, pH 7.5), stained with ethidium bromide (40 μl, 50 μg/ml), and observed under a fluorescence microscope equipped with a Komet 5.5 image analyzer (Kinetic Imaging Ltd., Nottingham, UK). The percentage of total cellular fluorescence in the comet tails and the tail lengths of 50 cells per slide were recorded.

Lipid peroxidation assay

Lipid peroxidation was assayed by colorimetric detection of 8-isoprostane, a stable end-product of lipid peroxidation, in the conditioned medium of HaCaT cells (Beauchamp *et al*., 2002). A commercial enzyme immune assay (Cayman Chemical, Ann Arbor, MI, USA) was used according to the manufacturer's instructions to detect 8-isoprostane levels.

Lipid peroxidation was also assessed by using DPPP as a probe (Okimotoa *et al*., 2000). DPPP reacts with lipid hydroperoxides to yield a fluorescent product, DPPP oxide (DPPP=O), thereby providing an indication of oxidative membrane damage. Cells were treated with GPF (20 μM) for 1 h, followed by exposure to H_2O_2 (1 mM). Five hours later, the cells were incubated with DPPP (20 μM) for 30 min in the dark. Images of DPPP=O fluorescence were captured by using a Zeiss Axiovert 200 inverted microscope at an excitation wavelength of 351 nm and an emission wavelength of 380 nm. The intensity of the DPPP=O fluorescence was then quantified.

Protein carbonyl formation

Cells were treated with GPF (20 μM) for 1 h, followed by the addition of H_2O_2 (1 mM) and further incubation for 36 h. The amount of protein carbonyl formation was determined by using an Oxiselect™ protein carbonyl enzyme-linked immunosorbent assay (ELISA) kit (Cell Biolabs, San Diego, CA, USA) according to the manufacturer's instructions.

Statistical analysis

All measurements were performed in three independent experiments, and all values are expressed as the mean ± the standard error (SE). The results were subjected to an analysis

of variance (ANOVA) and Tukey's post hoc test to analyze differences between conditions. In each case, a p value<0.05 was considered statistically significant.

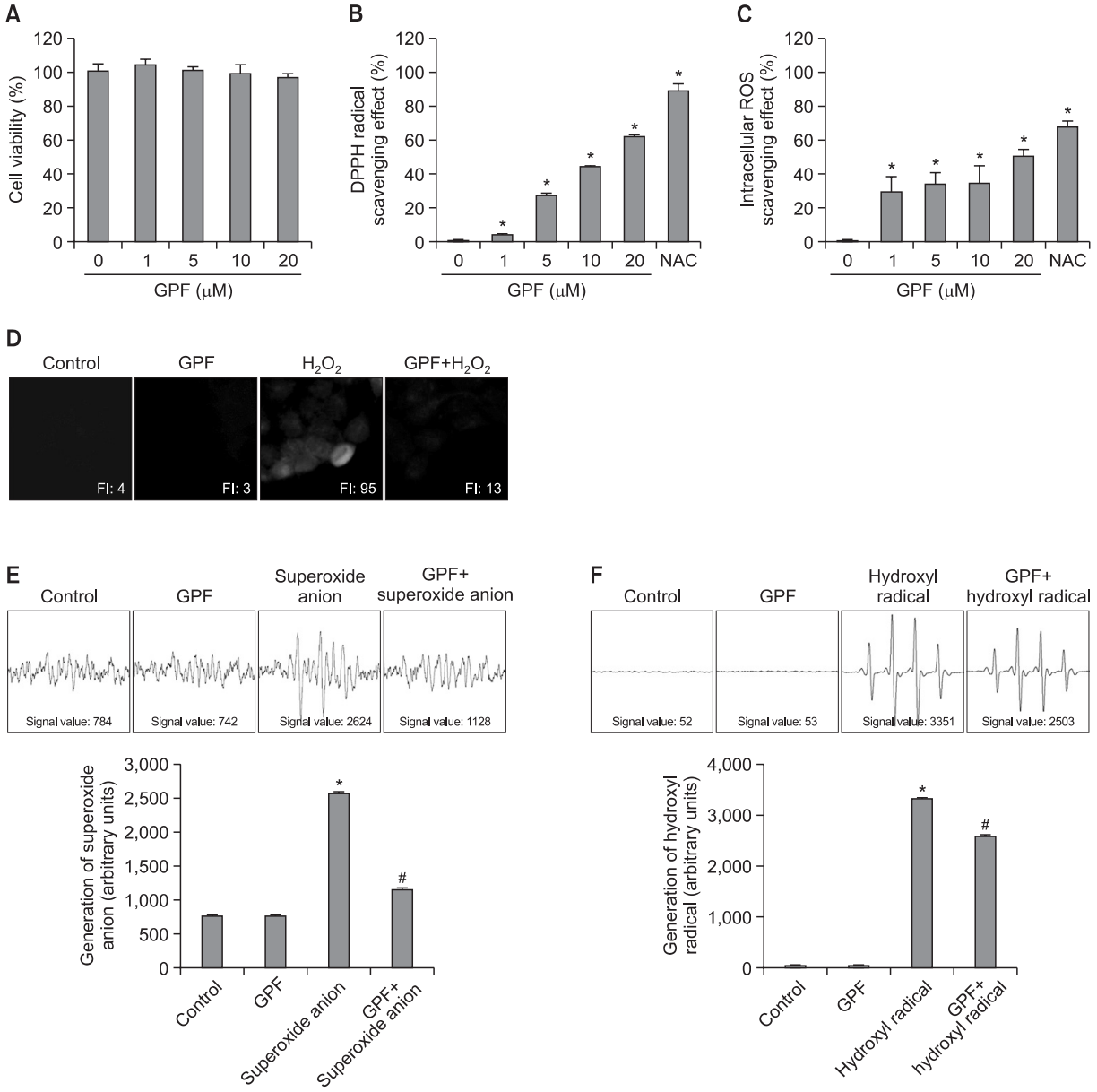

Fig. 2. GPF attenuates ROS generation in HaCaT keratinocytes and exhibits antiradical activity. (A) GPF (0, 1, 5, 10, or 20 μM) or NAC (2 mM) was added to HaCaT cells. After 16 h, cell viability was determined by the MTT assay. (B) Levels of the DPPH radical scavenged by various concentrations of GPF were measured spectrophotometrically at 520 nm. (C) HaCaT cells were treated with GPF (0, 1, 5, 10, or 20 μM) or NAC (2 mM), and H_2O_2 (1 mM) was added to the plate 1 h later. Following a 30 min incubation and DCF-DA staining, the generation of intracellular ROS was detected by using a spectrofluorometer. (D) Representative confocal images illustrate that the fluorescence intensity of DCF produced from DCF-DA by ROS was elevated in H_2O_2-treated HaCaT cells compared with control, untreated cells. GPF had no effect on its own, but lowered the fluorescence intensity of DCF in H_2O_2-treated cells. FI, fluorescence intensity. (E) The superoxide anion generated by the xanthine/xanthine oxidase system was reacted with DMPO, and the resulting DMPO/•OOH adducts were detected by ESR spectrometry. The results are expressed as representative peak data (control=PBS+DMPO, GPF=PBS+GPF+DMPO, superoxide anion=PBS+xanthine+xanthine oxidase+DMPO, GPF+superoxide anion=PBS+GPF+xanthine+xanthine oxidase+DMPO). (F) The hydroxyl radical generated by the Fenton reaction (H_2O_2+$FeSO_4$) was reacted with DMPO, and the resulting DMPO/•OH adducts were detected by ESR spectrometry. The results are expressed as representative peak data (control=PBS+DMPO, GPF=PBS+GPF+DMPO, hydroxyl radical=PBS+$FeSO_4$+H_2O_2+DMPO, GPF+hydroxyl radical=PBS+GPF+$FeSO_4$+H_2O_2+DMPO). All measurements were performed in three independent experiments. *Significantly different from control (p<0.05), #Significantly different from superoxide anion or hydroxyl radical (p<0.05).

RESULTS

GPF scavenges ROS induced by H_2O_2 in HaCaT keratinocytes

Human HaCaT keratinocytes were treated with GPF at concentrations ranging from 0 to 20 μM, and cell viability was determined 24 h later via the MTT assay. The corresponding values in untreated control and GPF-treated cells were all approximately 100%, consistent with the lack of cytotoxicity for GPF (Fig. 2A).

The scavenging activity of GPF against the DPPH radical was next evaluated in a cell-free system to confirm its antiradical activity. GPF scavenged the DPPH radical in a concentration-dependent manner, with 4% of the radicals scavenged at 1 μM, 27% at 5 μM, 44% at 10 μM, and 62% at 20 μM (Fig. 2B). The corresponding value was 89% for NAC (2 mM), a powerful antioxidant that is well known for its ability to minimize oxidative stress (Kerksick and Willoughby, 2005) (Fig. 2B). Furthermore, GPF dose-dependently scavenged H_2O_2-induced intracellular ROS in HaCaT keratinocytes, with 29% of the radicals scavenged at 1 μM, 33% at 5 μM, 35% at 10 μM, and 51% at 20 μM, vs. 68% for NAC (Fig. 2C). Thus, 20 μM of GPF was chosen as the optimal concentration for further study.

The antiradical activity of GPF was also evaluated via confocal microscopy after DCF-DA staining of HaCaT cells. The high fluorescence intensity of the DCF product generated by H_2O_2-induced ROS (fluorescence intensity, 95) was significantly decreased by pretreatment with 20 μM GPF (fluorescence intensity, 13), but GPF by itself had no effect on ROS production relative to untreated control cells (Fig. 2D).

Next, we investigated the scavenging effects of GPF against the superoxide anion and the hydroxyl radical by using ESR spectrometry. The superoxide anion signal was increased to a value of 2624 in the xanthine/xanthine oxidase system, compared with a value of 784 and 742 in the blank control (PBS+DMPO) and the GPF-only control (PBS+DMPO+GPF), respectively (Fig. 2E). However, GPF significantly decreased the superoxide anion signal in the xanthine/xanthine oxidase system to 1128. GPF also decreased the hydroxyl radical signal in the Fenton reaction system (H_2O_2+$FeSO_4$) from 3351 to 2503 (Fig. 2F). The values for the blank control and GPF-only control were 52 and 53, respectively. The results of Figure 2 thus demonstrate that GPF possesses efficient antiradical activity against the DPPH radical, intracellular ROS, the superoxide anion, and the hydroxyl radical.

GPF protects HaCaT keratinocytes from apoptosis provoked by H_2O_2

H_2O_2 is implicated in several physiological processes, including apoptosis (Antunes and Cadenas, 2001), a type of programmed cell death. Therefore, we assessed the protective effects of GPF on cell survival in H_2O_2-treated HaCaT keratinocytes. Cells were treated with GPF, NAC, H_2O_2, GPF+H_2O_2, or NAC+H_2O_2, and cell viability was determined 24 h later by the MTT assay. Cell viability in the presence of GPF+H_2O_2 was significantly increased to 73% from a value of 66% in the H_2O_2-only treatment group (Fig. 3A). NAC similarly enhanced cell viability in H_2O_2-treated cells. The corresponding values in untreated control, GPF-treated, and NAC-treated cells were all approximately 100% (Fig. 3A), consistent with the lack of cytotoxicity for GPF shown in Fig. 2A.

Dynamic changes in the compaction of nuclear chromatin are characteristic of apoptosis (Wyllie *et al*., 1984). Nuclear fragmentation with concomitant apoptotic body formation was visualized in HaCaT keratinocytes by Hoechst 33342 staining and fluorescence microscopy. Cell images and quantitative histograms demonstrated obvious nuclear fragmentation in the H_2O_2-treated cells (apoptotic index 23) relative to untreated control, GPF-treated, or NAC-treated cells (Fig. 3B). Conversely, nuclear fragmentation in H_2O_2-treated cells was dramatically reduced by pretreatment with GPF or NAC (apoptotic index 15 and 12, respectively). These observations indicate that GPF may rescue HaCaT keratinocytes from cell death resulting from H_2O_2-provoked apoptosis.

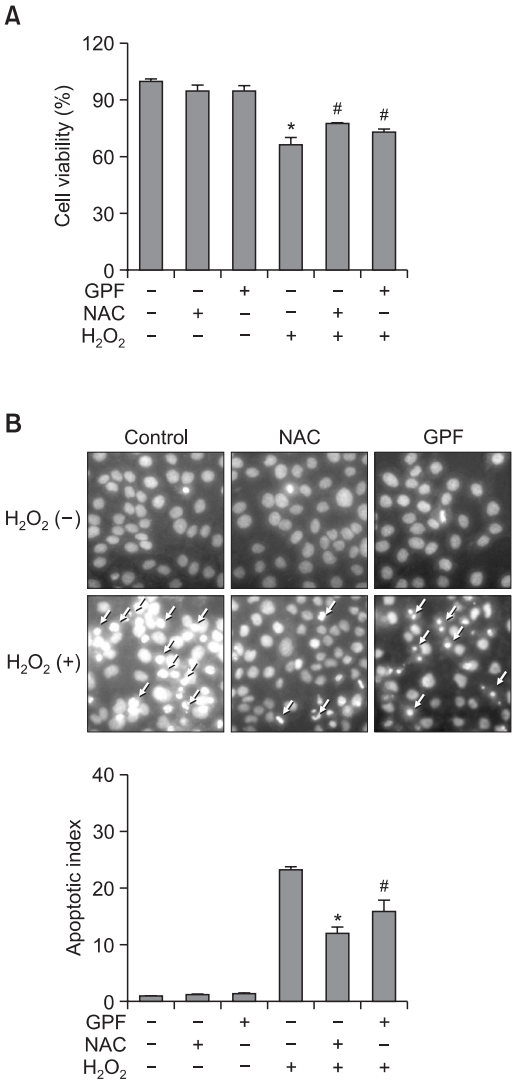

Fig. 3. GPF prevents H_2O_2-induced apoptosis in HaCaT keratinocytes. (A) HaCaT cells were treated with GPF (20 μM) or NAC (2 mM) and exposed to H_2O_2 (1 mM) 1 h later. After incubation for 24 h, cell viability (expressed as a percentage of total cells) was determined by the MTT assay. (B) Apoptotic bodies (arrows) were observed by fluorescence microscopy and quantified in cells stained with Hoechst 33342. All measurements were performed in three independent experiments. *Significantly different from control cells (p<0.05), #Significantly different from H_2O_2-treated cells (p<0.05).

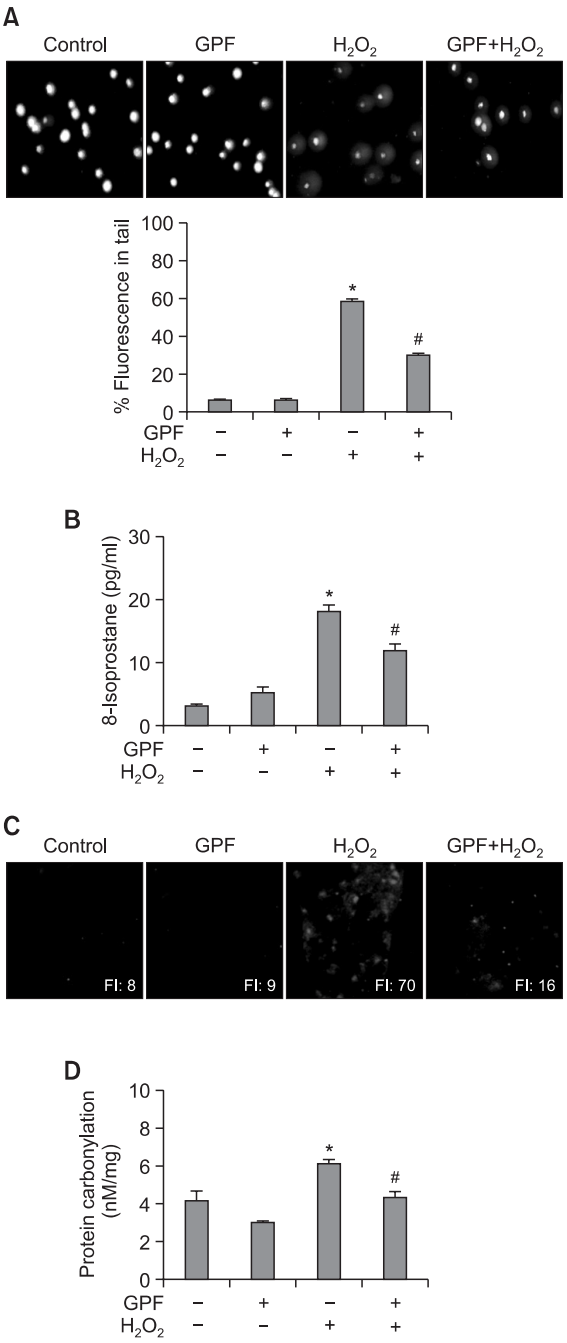

Fig. 4. GPF protects HaCaT keratinocytes against H_2O_2-induced oxidative DNA, lipid, and protein damage. HaCaT cells were treated with GPF (20 μM) for 1 h and then exposed to H_2O_2 (1 mM). (A) The comet assay was performed to assess DNA damage. Representative images and the percentage of cellular fluorescence within the comet tail are shown. Lipid peroxidation was assayed by (B) measuring 8-isoprostane levels in the conditioned medium and (C) detecting lipid hydroperoxide formation via fluorescence microscopy after reaction with DPPP. (D) Protein oxidation was assayed by measuring carbonyl formation. All measurements were performed in three independent experiments. *Significantly different from control cells (p<0.05), #Significantly different from H_2O_2-treated cells (p<0.05).

GPF attenuates H_2O_2-generated macromolecular damage in HaCaT keratinocytes

Disturbance of the balance between antioxidant defense systems and the production of H_2O_2 and other ROS produces oxidative stress, resulting in DNA strand breaks and considerable DNA damage (Hoffmann *et al*., 1984). DNA strand breaks are visualized in microscopic images as comets, where the DNA tail length directly reflects the intensity of the damage. Accordingly, we performed an alkaline comet assay in H_2O_2-treated HaCaT cells to explore the protective effects of GPF on keratinocyte DNA. H_2O_2 dramatically increased DNA tail lengths in fluorescence microscopy images, as well as the percentage of cellular DNA in the nuclear tails (Fig. 4A). However, GPF pretreatment (20 μM) significantly reduced the percentage of cellular DNA in the tails from 58% to 29%. By contrast, GPF alone had no effect on the DNA lesions compared with the untreated control. These results demonstrate that GPF attenuates DNA damage in HaCaT cells following exposure to H_2O_2.

Elevated ROS levels also release peroxidative forms of reactive iron, which in turn drive lipid peroxidation by eroding protective sacrificial antioxidants (Gutteridge, 1995). Lipid peroxidation can be monitored by measuring the amount of 8-isoprostane secreted into the conditioned medium of cultured cells. In the present study, GPF alone created a slight but insignificant increase in 8-isoprostane levels in HaCaT keratinocytes relative to untreated control cells (Fig. 4B). Nevertheless, GPF pretreatment prevented the significant increase in 8-isoprostane levels provoked by H_2O_2. The fluorescence intensity of DPPP, which reacts with lipid hydroperoxides to produce the highly fluorescent product, DPPP oxide (DPPP=O) (Okimotoa *et al*., 2000), was also notably enhanced in H_2O_2-treated compared with untreated control cells (Fig. 4C). However, GPF markedly decreased DPPP=O fluorescence, consistent with the results of the 8-isoprostane assay.

Finally, protein carbonylation is a biomarker of oxidative stress-induced protein damage (Dalle-Donne *et al*., 2003). The protein carbonyl level was significantly increased in H_2O_2-treated HaCaT keratinocytes relative to untreated control cells (Fig. 4D). By contrast, GPF prevented H_2O_2-induced protein carbonyl formation, analogous to its protective actions against DNA strand breaks and lipid peroxidation.

DISCUSSION

Paeoniflorin, a monoterpene glucoside, is one of the principle active components in Paeoniae Radix. Paeoniflorin is a well known extracellular ROS scavenger that exerts cytoprotective effects against ^{60}Co-ray-induced oxidative damage in thymocytes (Li *et al*., 2007). Moreover, paeoniflorin protects retinal pigment epithelium cells from oxidative stress by suppressing ROS production, caspase-3 activity, and p38 and extracellular-regulated kinase function, all of which are essential signaling pathway components in H_2O_2-induced cell death (Wankun *et al*., 2011).

GPF is a derivative of paeoniflorin and a product of the chemical reaction between paeoniflorin and gallic acid. GPF is isolated as a galloylated monoterpene glucoside. Intriguingly, gallic acid exhibits significant scavenging activity against the DPPH radical and inhibits lipid peroxidation and oxidative DNA damage, all without exhibiting any pro-oxidant activity

(Lee *et al*., 2005). Hence, putative antioxidant properties can logically be ascribed to GPF. Indeed, Matsuda and colleagues (2001) confirmed that GPF can efficiently scavenge the DPPH radical. However, our investigation is the first to demonstrate that GPF can also prevent H_2O_2-stimulated production of excess intracellular ROS and rescue human HaCaT keratinocytes from H_2O_2-induced macromolecular cell injury, and perhaps even cell death.

Our initial goal was to determine the most suitable concentration of GPF for study. Taking into account the bioactive actions of the compound on cell viability and its antiradical capacity against both the DPPH radical and intracellular ROS, a concentration of 20 μM was chosen as optimal. In addition, it is worth mentioning that no cytotoxicity was associated with any concentration of GPF employed, which is essential if it is to be used as a therapeutic agent to overcome oxidative stress.

Excessive levels of ROS can lead to oxidative stress by overwhelming cellular and tissue antioxidant defense systems. H_2O_2 is unique among the ROS family members because it is a metabolite of O_2^- and a partial generator of •OH in living organisms (Farber, 1994). The yield of •OH by treatment of H_2O_2 is usually depending on the split of oxygen-oxygen bond of H_2O_2 by the addition of one electron. The best known sources of electrons for the reduction of H_2O_2 are transition metal cations, particularly ferrous ions and cuprous ions. Ferrous ion reduces H_2O_2 to form •OH and OH^- with accompanying formation of ferric ion (Pignatello *et al*., 2006). The detailed mechanism of H_2O_2-stimulated O_2^- generation is not totally understood until now. The xanthine oxidase pathway for intracellular O_2^- production accounts for approximately 40% of the total cellular O_2^- generated in endothelial cells after stimulation with H_2O_2 (Carter *et al*., 1994). Moreover, exposure of endothelial cells to H_2O_2 increased production of O_2^- likely derived from xanthine oxidase, NADPH-oxidase and mitochondria (Witting *et al*., 2008). Hence, treatment of H_2O_2 increases the intracellular ROS levels directly by itself and also indirectly by promoting the generation of other kinds of ROS.

We selected H_2O_2 as an oxidative inducer of ROS in a HaCaT keratinocyte model due to its high diffusion capacity and rapid membrane permeability. Furthermore, the mechanisms by which H_2O_2 induces alterations in cellular components and regulates cell fate are well understood (Hampton and Orrenius, 1998; Nguyen *et al*., 2013), which makes this ROS particularly attractive for study. In the present investigation, GPF (20 μM) significantly reversed H_2O_2-induced intracellular ROS generation. Furthermore, GPF showed strong antiradical activity against the superoxide radical and the hydroxyl radical, as detected by ESR in cell-free systems. Thus, the current study successfully established the free radical- and ROS-scavenging capacity of GPF.

Nowadays, there is growing awareness that oxidative stress plays an important role in the pathogenesis of various clinical conditions and diseases. At the molecular level, oxidative stress is characterized by ROS-mediated injury to DNA, lipids, and proteins (Ray *et al*., 2012). Of these, oxidative damage to DNA is perhaps the most critical to cell survival and causes the most grievous harm to cells. ROS-induced oxidative DNA damage includes a range of specifically oxidized purines and pyrimidines, alkali labile sites, single strand breaks, and other instabilities. These lesions are either formed directly or indirectly during the repair process (Waris and Ahsan, 2006). The extent of DNA damage due to alkali labile sites and single strand breaks is commonly investigated by using the comet assay (Horváthová *et al*., 1998). Indeed, we used the comet assay in this investigation to evaluate the DNA-protective actions of GPF.

Secondarily, elevated ROS levels culminate in oxidative damage to lipids in the form of lipid peroxidation. Lipid peroxidation is detected by assaying for thiobarbituric acid reactive substances, for the lipid hydroperoxides themselves, or for their degradation products, such as malondialdehyde and 4-hydroxy-2-nonenal. DPPP reacts with hydroperoxides in a stoichiometric manner to yield DPPP=O, providing a suitable method for the quantitative measurement of oxidative lipid damage (Okimotoa *et al*., 2000). Furthermore, 8-isoprostane, an isoprostane produced via the random oxidation of tissue phospholipids by oxygen radicals, is a proposed biomarker for antioxidant deficiency and oxidative stress (Morrow *et al*., 1995). Hence, the quantification of 8-isoprostane levels, like DPPP=O fluorescence, provides a reliable measure of H_2O_2-provoked injury to cell membranes.

Finally, protein oxidation occurs as a result of covalent modification and is promoted either directly by ROS or indirectly by reaction with secondary by-products of oxidative stress. The most commonly observed products of protein oxidation in biological samples are the carbonyl derivatives of proline, arginine, lysine, and threonine. These derivatives are chemically stable and serve as markers of oxidative stress for most types of ROS (Shacter, 2000; Dalle-Donne *et al*., 2003), including H_2O_2. Our present research showed that GPF significantly prevented H_2O_2-induced macromolecular damage to HaCaT keratinocytes by decreasing protein carbonylation, DNA lesions, and the generation of both 8-isoprostane and DPPP=O, substantiating the cytoprotective effect of GPF on human keratinocytes against oxidative stress.

Thus far, it is well-acknowledged that ROS-provoked oxidative stress can ultimately kill cells via necrosis and/or apoptosis. Apoptosis is a complex process characterized by cell shrinkage, chromatin condensation, internucleosomal DNA fragmentation, and the formation of apoptotic bodies. Increased ROS levels effectively initiate apoptosis through a variety of overlapping signaling pathways and cascades that are still under study. The addition of exogenous H_2O_2 is sufficient to trigger the apoptotic program, with different concentrations required depending on the cell type investigated (Hampton and Orrenius, 1998; Chandra *et al*., 2000). We found that GPF reduced nuclear fragmentation and the formation of apoptotic bodies in H_2O_2-treated HaCaT keratinocytes, confirming that GPF prevents ROS-mediated programmed cell death via the attenuation of oxidative stress. Cells treated with NAC, a widely used ROS inhibitor, have also been shown to reduce programmed cell death. Moreover, GPF reversed the significant reduction in cell viability promoted by H_2O_2. As a result, it provided that GPF possessed the ability to attenuate the intracellular ROS generation. However, the antioxidant capacity of GPF in terms of other ROS generators such as UVB needs to be investigated in next study.

In summary, this study identified GPF as an antioxidant with the ability to scavenge free radicals, and especially intracellular ROS in human HaCaT keratinocytes. Moreover, GPF prevented cell damage resulting from H_2O_2 exposure and also increased HaCaT cell survival. These data suggest that GPF might find utility as a therapeutic agent for the management

of ROS-linked clinical conditions and disorders. However, achievement of this goal will require further investigation to elucidate the detailed mechanism by which GPF mitigates apoptosis, as well as the impact of GPF on different cell lines and in animal models.

ACKNOWLEDGMENTS

This work was supported by the National Research Foundation of Korea Grant funded by the Korean Government (MEST) (NRF-C1ABA001-2011-0021037).

REFERENCES

Alfadda, A. A. and Sallam, R. M. (2012) Reactive oxygen species in health and disease. *J. Biomed. Biotechnol.* **2012**, 936486.

Antunes, F. and Cadenas, E. (2001) Cellular titration of apoptosis with steady state concentrations of H_2O_2: submicromolar levels of H_2O_2 induce apoptosis through Fenton chemistry independent of the cellular thiol state. *Free Radic. Biol. Med.* **30**, 1008-1018.

Beauchamp, M. C., Letendre, É. and Renier, G. (2002) Macrophage lipoprotein lipase expression is increased in patients with heterozygous familial hypercholesterolemia. *J. Lipid Res.* **43**, 215-222.

Bickers, D. R. and Athar, M. (2006) Oxidative stress in the pathogenesis of skin disease. *J. Invest. Dermatol.* **126**, 2565-2575.

Brambilla, D., Mancuso, C., Scuderi, M. R., Bosco, P., Cantarella, G., Lempereur, L., Di Benedetto, G., Pezzino, S. and Bernardini, R. (2008) The role of antioxidant supplement in immune system, neoplastic, and neurodegenerative disorders: a point of view for an assessment of the risk/benefit profile. *Nutr. J.* **7**, 29

Cai, H. (2005) Hydrogen peroxide regulation of endothelial function: origins, mechanisms, and consequences. *Cardiovasc. Res.* **68**, 26-36.

Carmichael, J., DeGraff, W. G., Gazdar, A. F., Minna, J. D. and Mitchell, J. B. (1987) Evaluation of a tetrazolium-based semiautomated colorimetric assay: assessment of chemosensitivity testing. *Cancer Res.* **47**, 936-942.

Carter, W., Narayanan, P. K. and Robinson, J. (1994) Intracellular hydrogen peroxide and superoxide anion detection in endothelial cells. *J. Leukoc. Biol.* **55**, 253-258.

Chandra, J., Samali, A. and Orrenius, S. (2000) Triggering and modulation of apoptosis by oxidative stress. *Free Radic. Biol. Med.* **29**, 323-333.

Dalle-Donne, I., Rossi, R., Giustarini, D., Milzani, A. and Colombo, R. (2003) Protein carbonyl groups as biomarkers of oxidative stress. *Clin. Chim. Acta* **329**, 23-38.

Farber, J. L. (1994) Mechanisms of cell injury by activated oxygen species. *Environ. Health Perspect.* **102**, 17-24.

Gutteridge, J. (1995) Lipid peroxidation and antioxidants as biomarkers of tissue damage. *Clin. Chem.* **41**, 1819-1828.

Haigis, M. C. and Yankner, B. A. (2010) The aging stress response. *Mol. Cell* **40**, 333-344.

Halliwell, B. (1999) Oxygen and nitrogen are pro-carcinogens. Damage to DNA by reactive oxygen, chlorine and nitrogen species: measurement, mechanism and the effects of nutrition. *Mutat. Res.* **443**, 37-52.

Halliwell, B. (2007) Oxidative stress and cancer: have we moved forward? *Biochem. J.* **401**, 1-11.

Hampton, M. B. and Orrenius, S. (1998) Redox regulation of apoptotic cell death. *BioFactors* **8**, 1-5.

Hoffmann, M. E., Mello-Filho, A. C. and Meneghini, R. (1984) Correlation between cytotoxic effect of hydrogen peroxide and the yield of DNA strand breaks in cells of different species. *Biochim. Biophys. Acta* **781**, 234-238.

Horváthová, E., Slameňová, D., Hlinčíková, L., Mandal, T. K., Gábelová, A. and Collins, A. R. (1998) The nature and origin of DNA single-strand breaks determined with the comet assay. *Mutat. Res.* **409**, 163-171.

Kang, S. S., Shin, K. H. and Chi, H. J. (1991) Galloylpaeoniflorin, a new acylated monoterpene glucoside from paeony root. *Arch. Pharm. Res.* **14**, 52-54.

Kerksick, C. and Willoughby, D. (2005) The antioxidant role of glutathione and N-acetyl-cysteine supplements and exercise-induced oxidative stress. *J. Int. Soc. Sports Nutr.* **2**, 38-44.

Kohno, M., Mizuta, Y., Kusai, M., Masumizu, T. and Makino, K. (1994) Measurements of superoxide anion radical and superoxide anion scavenging activity by electron spin resonance spectroscopy coupled with DMPO spin trapping. *Bull. Chem. Soc. Jpn.* **67**, 1085-1090.

Lee, S. C., Kwon, Y. S., Son, K. H., Kim, H. P. and Heo, M. Y. (2005) Antioxidative constituents from Paeonia lactiflora. *Arch. Pharm. Res.* **28**, 775-783.

Li, C. R., Zhou, Z., Zhu, D., Sun, Y. N., Dai, J. M. and Wang, S. Q. (2007) Protective effect of paeoniflorin on irradiation-induced cell damage involved in modulation of reactive oxygen species and the mitogen-activated protein kinases. *Int. J. Biochem. Cell Biol.* **39**, 426-438.

Li, L., Abe, Y., Kanagawa, K., Usui, N., Imai, K., Mashino, T., Mochizuki, M. and Miyata, N. (2004) Distinguishing the 5,5-dimethyl-1-pyrroline N-oxide (DMPO)-OH radical quenching effect from the hydroxyl radical scavenging effect in the ESR spin-trapping method. *Anal. Chim. Acta* **512**, 121-124.

Liu, B., Jian, Z., Li, Q., Li, K., Wang, Z., Liu, L., Tang, L., Yi, X., Wang, H., Li, C. and Gao, T. (2012) Baicalein protects human melanocytes from H2O2-induced apoptosis via inhibiting mitochondria-dependent caspase activation and the p38 MAPK pathway. *Free Radic. Biol. Med.* **53**, 183-193.

Maioli, E., Greci, L., Soucek, K., Hyzdalova, M., Pecorelli, A., Fortino, V. and Valacchi, G. (2009) Rottlerin inhibits ROS formation and prevents NFκB activation in MCF-7 and HT-29 cells. *J. Biomed. Biotechnol.* **2009**, 742936.

Matsuda, H., Ohta, T., Kawaguchi, A. and Yoshikawa, M. (2001) Bioactive constituents of chinese natural medicines. VI. Moutan cortex. (2): structures and radical scavenging effects of suffruticosides A, B, C, D, and E and galloyl-oxypaeoniflorin. *Chem. Pharm. Bull.* **49**, 69-72.

Meyers, D. G., Maloley, P. A. and Weeks, D. (1996) Safety of antioxidant vitamins. *Arch. Intern. Med.* **156**, 925-935.

Morrow, J. D., Frei, B., Longmire, A. W., Gaziano, J. M., Lynch, S. M., Shyr, Y., Strauss, W. E., Oates, J. A. and Roberts, L. J. (1995) Increase in circulating products of lipid peroxidation (F2-isoprostanes) in smokers-smoking as a cause of oxidative damage. *N. Engl. J. Med.* **332**, 1198-1203.

Motterlini, R., Foresti, R., Bassi, R. and Green, C. J. (2000) Curcumin, an antioxidant and anti-inflammatory agent, induces heme oxygenase-1 and protects endothelial cells against oxidative stress. *Free Radic. Biol. Med.* **28**, 1303-1312.

Nguyen, C. N., Kim, H. E. and Lee, S. G. (2013) Caffeoylserotonin protects human keratinocyte HaCaT cells against H_2O_2-induced oxidative stress and apoptosis through upregulation of HO-1 expression via activation of the PI3K/Akt/Nrf2 pathway. *Phytother. Res.* doi: 10. 1002/ptr. 4931. [Epub ahead of print]

Okimotoa, Y., Watanabe, A., Niki, E., Yamashita, T. and Noguchi, N. (2000) A novel fluorescent probe diphenyl-1-pyrenylphosphine to follow lipid peroxidation in cell membranes. *FEBS Lett.* **474**, 137-140.

Paravicini, T. M. and Touyz, R. M. (2006) Redox signaling in hypertension. *Cardiovasc. Res.* **71**, 247-258.

Patel, V. P. and Chu, C. T. (2011) Nuclear transport, oxidative stress, and neurodegeneration. *Int. J. Clin. Exp. Pathol.* **4**, 215-229.

Pignatello, J. J., Oliveros, E. and MacKay, A. (2006) Advanced oxidation processes for organic contaminant destruction based on the Fenton reaction and related chemistry. *Crit. Rev. Environ. Sci. Technol.* **36**, 1-84.

Poljsak, B. (2011) Strategies for reducing or preventing the generation of oxidative stress. *Oxid. Med. Cell. Longev.* **2011**, 194586.

Pryor, W. A. (2000) Vitamin E and heart disease: Basic science to clinical intervention trials. *Free Radic. Biol. Med.* **28**, 141-164.

Rajagopalan, R., Ranjan, S. K. and Nair, C. K. K. (2003) Effect of vin-

blastine sulfate on γ-radiation-induced DNA single-strand breaks in murine tissues. *Mutat. Res.* **536**, 15-25.

Ray, P. D., Huang, B. W. and Tsuji, Y. (2012) Reactive oxygen species (ROS) homeostasis and redox regulation in cellular signaling. *Cell. Signal*. **24**, 981-990.

Rosenkranz, A. R., Schmaldienst, S., Stuhlmeier, K. M., Chen, W., Knapp, W. and Zlabinger, G. J. (1992) A microplate assay for the detection of oxidative products using 2, 7′-dichlorofluorescin-diacetate. *J. Immunol. Methods* **156**, 39-45.

Scandalios, J. G. (2002) The rise of ROS. *Trends Biochem. Sci.* **27**, 483-486.

Shacter, E. (2000) Quantification and significance of protein oxidation in biological samples. *Drug Metab. Rev.* **32**, 307-326.

Singh, N. P. (2000) Microgels for estimation of DNA strand breaks, DNA protein crosslinks and apoptosis. *Mutat. Res.* **455**, 111-127.

Srivastava, A., Jagan Mohan Rao, L. and Shivanandappa, T. (2012) A novel cytoprotective antioxidant: 4-Hydroxyisophthalic acid. *Food Chem.* **132**, 1959-1965.

Wankun, X., Wenzhen, Y., Min, Z., Weiyan, Z., Huan, C., Wei, D., Lvzhen, H., Xu, Y. and Xiaoxin, L. (2011) Protective effect of paeoniflorin against oxidative stress in human retinal pigment epithelium in vitro. *Mol. Vis.* **17**, 3512-3522.

Waris, G. and Ahsan, H. (2006) Reactive oxygen species: role in the development of cancer and various chronic conditions. *J. Carcinog.* **5**, 14.

Witting, P. K., Rayner, B. S., Wu, B.J., Ellis, N. A. and Stocker, R. (2008) Hydrogen peroxide promotes endothelial dysfunction by stimulating multiple sources of superoxide anion radical production and decreasing nitric oxide bioavailability. *Cell. Physiol. Biochem.* **20**, 255-268.

Wyllie, A., Morris, R., Smith, A. and Dunlop, D. (1984) Chromatin cleavage in apoptosis: association with condensed chromatin morphology and dependence on macromolecular synthesis. *J. Pathol.* **142**, 67-77.